ELSEVIER

Journal of Organometallic Chemistry 541 (1997) 377–389

Journal of Organometallic Chemistry

Anchoring rhodium(I) on thiourea-functionalized silica xerogels and silsesquioxanes
Part II. Matrix effects on the selectivity in the hydroformylation of styrene [1,2]

Daniele Cauzzi [a], Mirco Costa [b], Luca Gonsalvi [a], Maria Angela Pellinghelli [a], Giovanni Predieri [a], Antonio Tiripicchio [a,*], Roberto Zanoni [c]

[a] *Dipartimento di Chimica Generale ed Inorganica, Chimica Analitica, Chimica Fisica, Università di Parma, Centro di Studio per la Strutturistica Diffrattometrica del CNR, Viale delle Scienze 78, I-43100 Parma, Italy*

[b] *Dipartimento di Chimica Organica e Industriale, Università di Parma, Viale delle Scienze 78, I-43100 Parma, Italy*

[c] *Dipartimento di Chimica, Università di Roma "La Sapienza", Piazzale Aldo Moro 5, I-00185 Roma, Italy*

Received 15 January 1997; accepted 19 January 1997

Abstract

Three thiourea-functionalized siloxane materials, $5SiO_2 \cdot SiO_{3/2}(CH_2)_3NHC(S)NHPh$ (XGphtu), $SiO_{3/2}(CH_2)_3NHC(S)NHPh$ (XGphtu*) and p-$\{SiO_{3/2}(CH_2)_3NHC(S)NH\}_2C_6H_4$ (XGphenditu*) were prepared. They are able to anchor Rh(I) species giving supported complexes that are very active recoverable catalysts for the hydroformylation of styrene. Some of these materials show regioselectivity variation when used in consecutive catalytic runs. The recovered catalysts have been investigated by XPS and EDX and the change in regioselectivity has been ascribed to matrix effects. In fact, the surface rhodium leaching apparently forces the catalytic process to move in the inside of the materials causing the substrate to experience the inner matrix environment. Furthermore, the non-siloxanized thioureas PhNHC(S)NHPh (Phtu) and p-$\{PrNHC(S)NH\}_2C_6H_4$ (Phenditu), which give discrete molecular Rh(I) complexes, were studied as models for the surface binding functions. The structure of [Rh(cod)Cl(Phtu)] (cod = 1,5-cyclooctadiene) has been determined by X-ray diffraction methods. © 1997 Published by Elsevier Science S.A.

Keywords: Rhodium; Crystal structure; Hydroformylation; Thiourea ligands; Silica xerogels; Silsesquioxanes

1. Introduction

Recently, we studied the catalytic activity, in the hydroformylation of styrene, of thiourea-rhodium complexes [1] anchored to inorganic–organic hybrid materials [2] obtained by the sol–gel method [3]. In particular, a 'function-diluted' xerogel (XGbztu) with a given S/Si ratio was obtained by sol–gel processing the 'siloxanized' benzoylthiourea $(EtO)_3Si(CH_2)_3NHC(S)NHC(O)Ph$ (Sibztu) with tetraethoxysilane (TEOS) as cross-linking agent. A 'superfunctionalized' silsesquioxane material (S/Si ratio 1:1, XGbztu*) was also prepared by reacting $[SiO_{3/2}(CH_2)_3NH_2]_n$ (mainly a mixture of oligomers with $n = 8$, 10) with benzoyl isothiocyanate alone. All these products are able to bind the Rh(cod)Cl moiety (cod = 1,5-cyclooctadiene) through sulphur coordination, forming metal complexes tethered to the surface which behave as heterogenized homogeneous (hybrid) catalysts [4] in the hydroformylation of styrene. Interestingly, for the function-diluted rhodium catalyst (derived from XGbztu) a significant change in selectivity was observed by recycling the catalyst. Notwithstanding the high catalytic activity of these systems, the benzoylthiourea function gradually decomposes just in the function-diluted material, so that more robust ligands are needed to prevent this drawback.

In this paper, we report the results obtained by using two kinds of support containing a simpler thiourea

* Corresponding author. Fax: (+39) 521 905557; e-mail: tiri@ipruniv.cce.unipr.it.

[1] Dedicated to Professor Gottfried Huttner on the occasion of his 60th birthday.

[2] Part I, see Ref. [1].

PII S0022-328X(97)00089-2

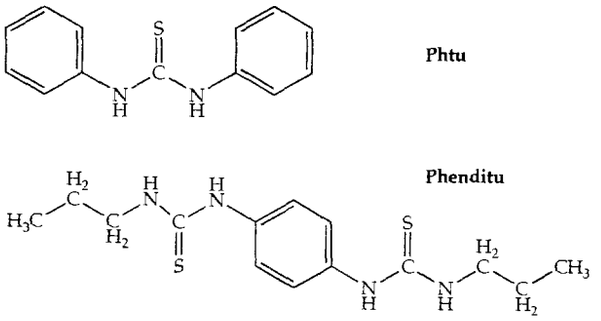

Scheme 1.

function, namely the 'superfunctionalized' silsesquioxane derivatives $[SiO_{3/2}(CH_2)_3NHC(S)NHPh]_n$ (XGphtu*) and $[p\text{-}\{SiO_{3/2}(CH_2)_3NHC(S)NH\}_2C_6H_4]_n$ (XGphenditu*) and the 'function-diluted' xerogel $5SiO_2 \cdot SiO_{3/2}(CH_2)_3NHC(S)NHPh$ (XGphtu). Actually, the catalysts, obtained by anchoring rhodium(I) on these supports, were found to be more stable than the previous ones, under the hydroformylation conditions. Furthermore, the same trend of the change in the regioselectivity found for the XGbztu system [1], was observed in the case of XGphtu and XGphenditu*. The branched (*iso*-) to linear (*n*-) aldehydes ratio increases depending on the number of times the same catalyst is reused, and this can be reasonably attributed to matrix effects.

Moreover, the corresponding 'non-siloxanized' thioureas PhNHC(S)NHPh (Phtu) and *p*-$\{PrNHC(S)NH\}_2C_6H_4$ (Phenditu) were synthesized and used to obtain discrete rhodium complexes as suitable models of the anchored species (Scheme 1).

2. Experimental details

2.1. Materials and analytical equipment

All the organic and organometallic reagents were pure commercial products. $[\{Rh(CO)_2Cl\}_2]$ was sublimed before use. $[SiO_{3/2}(CH_2)_3NH_2]_n$ was prepared as previously reported [1]. The solvents were reagent grade and were dried and distilled by standard techniques before use. All manipulations of rhodium compounds and reagents containing the triethoxysilyl group (before the sol–gel process) were carried out under dry nitrogen by means of standard Schlenk-tube techniques.

Elemental analyses (C, H, N, S) were performed with a Carlo Erba EA 1108 automated analyser. IR spectra were recorded on a Nicolet 5PC FT spectrometer. ^1H and ^{13}C NMR spectra were obtained with Bruker AC-100, AC-300 and CPX-200 instruments. Analytical GLC was carried out with a DANI 3900 chromatograph fitted with a methyl-silicone (OV101) coated capillary column. Energy dispersive X-ray (EDX) microanalyses were obtained with a JEOL 6400 EDS Tracor system for electron microscope microanalysis.

BET surface areas were measured using a Micromeritics 2200 equipment, from nitrogen absorption at the temperature of liquid nitrogen, after degassing the samples in a nitrogen steam at 423 K for about 1 h.

The hydroformylation reactions (and other reactions under pressure) were performed in a 50 ml stainless steel autoclave (Parr) equipped with a magnetic stirrer and thermostated (± 1 °C) in a silicone-oil bath (Heidolph). Yield and selectivity were determined by GLC using internal standards.

XPS spectra were run on a Vacuum Generators ESCALAB spectrometer, equipped with a hemispherical analyser operated in the fixed analyser transmission (FAT) mode, with a pass energy of 20 or 50 eV. Al K$\alpha_{1,2}$, or Mg K$\alpha_{1,2}$ photons ($h\nu = 1486.6$ and 1253.6 eV respectively) were used to excite photo-emission. The binding energy (BE) scale was calibrated by taking the Au $4f_{7/2}$ peak at 84.0 eV. Correction of the energy shift due to static charging of the samples was accomplished by referencing to the C(1s) line from the residual pump line oil contamination, taken at 285.0 eV. The accuracy of reported BEs was ± 0.2 eV, and the reproducibility of the results was within these values. XPS atomic ratios are relative values, intrinsically affected by a $\pm 10\%$ error. The spectra were collected by a DAC PDP 11/83 data system and processed by means of VG 5000 data handling software.

The AFM image was obtained by a Nanoscope IIIa (Digital Instruments), operating in contact mode; 200 μm silicon nitride cantilevers with Au-coated integral tips were used (force constant 0.06 N m^{-1}). Samples were prepared by breaking small monoliths of material, in such a way as to have a surface as flat as possible for easy engaging of the tip and free from any solid contaminant.

2.2. Preparations and reactions

2.2.1. Preparation of Phtu

1.45 g (10.73 mmol) of phenylisothiocyanate were added to a solution of 1 g (10.73 mmol) of aniline in 50 ml of ethanol. An exothermic reaction took place and a white precipitate was formed. The mixture was refluxed for 1 h, cooled at −30 °C and then filtered. The rough precipitate was washed with hexane to effectively eliminate dark impurities. The product was obtained as a white crystalline solid. Yield 98%. ^1H NMR ($CDCl_3$, 100 MHz, δ/ppm): 7.95 (s, br, 2H, NH), 7.4–7.2 (m, 10 H, Ph); IR (KBr, cm^{-1}): 3208s br, (νNH), 3037m, 3009m (νCH), 1557s br (ν_{as}NCN, B band), 631w (νCS, G band).

2.2.2. Preparation of Phenditu

2 g (18.5 mmol) of 1,4-diaminobenzene and 3.75 g (37 mmol) of propylisothiocyanate were dissolved in 50 ml of ethanol and then refluxed for 2 h, observing the formation of a white precipitate. The solvent was completely evaporated under vacuum. The rough white precipitate was filtered and washed with hexane to eliminate coloured impurities coming from the amine. The product was recrystallized from boiling methanol, giving crystals suitable for the X-ray structural analysis. Yield 75%. Elemental analysis (calcd for $C_{14}H_{22}N_4S_2$): C, 55.7 (54.2); H, 7.8 (7.1); N, 18.2 (18.0); S, 21.4 (20.7). IR (KBr, cm^{-1}): 3257m, 3177m, (νNH), 3002w, 2963w, 2933vw, 2875vw (νCH), 1549vs br, 1523s sh (ν_{as}NCN, B band), 654m (νCS, G band). ^{1}H NMR (DMSO-d_6, 100 MHz, δ/ppm): 9.4 (s, 2 H, N*H*C_6H_4); 7.7 (t, 2 H, N*H*Pr); 7.3 (s, 4 H, C_6H_4; 3.4 (dt, 4 H, NHCH_2); 1.5 (m, 4 H, CH_2); 0.9 (t, 6 H, CH_3).

2.2.3. Reaction of Phtu with [{Rh(cod)Cl}$_2$], preparation of [Rh(cod)Cl(Phtu)] (1)

In a Schlenk tube, 100 mg (0.203 mmol) of [{Rh(cod)Cl}$_2$] and 92.5 mg (0.406 mmol) of Phtu were dissolved in 10 ml of CH_2Cl_2 giving a yellow solution. After 1 h of reaction, one-half of the solvent was evaporated under vacuum and an equal volume of hexane was added. Upon cooling at −30 °C, yellow crystals suitable for X-ray structural analysis were obtained. Yield > 95%. Elemental analysis (calcd for $C_{21}H_{24}ClN_2RhS \cdot \frac{1}{2}CH_2Cl_2$): C, 51.8 (49.9); H, 4.9 (4.9); N, 5.4 (5.4); S, 6.3 (6.2). ^{1}H NMR ($CDCl_3$, 100 MHz, δ/ppm): 9.56 (s, br, 2 H, NH); 7.4–7.2 (m, 10 H, Ph); 4.21 (s, br, 4 H, CH=CH); 2.42–2.35 (m, 4 H, CH_2); 1.93–1.74 (m, 4 H, CH_2). ^{13}C NMR ($CDCl_3$, 100 MHz, δ/ppm): 177 (CS); 136, 129.5, 127.5, 125.5 (Ph), 81.5 (CH=CH), 31 (CH_2). IR (KBr cm^{-1}): 3356vw, 3276w (νNH), 3116w, 3083w (νCH arom.), 2983w, 2947m, 2877vw, 2831vw (νCH cod), 1556vs br (ν_{as}NCN, B band), 516w (νCS, G band).

2.2.4. Reaction of Phenditu with [{Rh(cod)Cl}$_2$], preparation of [{Rh(cod)Cl}$_2$(Phenditu)] (2)

68.2 mg (0.405 mmol) of Phenditu were dissolved in 20 ml of hot methanol under nitrogen and added to a solution of 200 mg (0.810 mmol) of [{Rh(cod)Cl}$_2$] in 20 ml of dichloromethane. A yellow precipitate formed. The solid was filtered and washed with dichloromethane. Yield 98%. Its insolubility in common deuterated organic solvents prevented recording of NMR spectra. Elemental analysis (calcd for $C_{30}H_{46}Cl_2N_4Rh_2S_2$): C, 45.10 (44.84); H, 5.91 (5.77); N, 7.03 (6.97); S, 8.10 (7.98). IR (KBr cm^{-1}): 3380vw sh, 3215s br (νNH), 2961w, 2931w (νCH), 2873w, 2832vw sh (νCH, cod), 1568vs br (ν_{as}NCN, B band), 518w (νCS, G band).

2.2.5. Reaction of Phtu with [{Rh(CO)$_2$Cl}$_2$], preparation of[Rh(CO)$_2$Cl(Phtu)] (3)

Compound **3** was previously characterized [5]. Here we report additional spectroscopic data for the sake of comparison. 117 mg (0.514 mmol) of Phtu and 100 mg (0.257 mmol) of [{Rh(CO)$_2$Cl}$_2$] were dissolved in 10 ml of CH_2Cl_2 under nitrogen. The yellow solution was stirred for 10 min and then hexane added. By cooling, a dark red oily product formed. By long drying under vacuum an unstable product was obtained and for this reason satisfactory elemental analysis was not obtained. IR (KBr, cm^{-1}): 3332m, 3210w br (νNH), 3058w 2925w (νCH), 2070vs, 1998vs (νCO), 1560s (ν_{as}NCN, B band), 515w (νCS, G band); IR (CH_2Cl_2, cm^{-1}) 2084s, 2014s (νCO). ^{1}H NMR ($CDCl_3$, 100 MHz, δ/ppm): 9.5 (s, br, 2 H, NH); 7.5–7.2 (m, 10 H, arom.).

2.2.6. Reaction of Phenditu with [{Rh(CO)$_2$Cl}$_2$], preparation of [{Rh(CO)$_2$Cl}$_2$(Phenditu)] (4)

In a Schlenk flask 100 mg (0.322 mmol) of Phenditu and 125 mg (0.322 mmol) of [{Rh(CO)$_2$Cl}$_2$] were refluxed in 50 ml of methanol for 1 h. The yellow solution was reduced in volume under vacuum and diethyl ether added. A yellow precipitate formed and was filtered and washed with ether. Yield 70%. Elemental analysis (calcd for $C_{18}H_{22}Cl_2N_4Rh_2S_2$): C, 29.88 (30.92); H, 3.31 (3.17); N, 7.59 (8.01); S, 9.21 (9.17). IR (KBr, cm^{-1}): 3223m (νNH), 2963m 2931m 2874w (νCH), 2072vs 2000vs (νCO), 1565s br (ν_{as}NCN, B band), 505vw (νCS, G band).

2.2.7. Reaction of Li[PhNC(S)NHPh] with [{Rh(CO)$_2$Cl}$_2$]

In a 150 ml Schlenk flask, 117.5 mg (0.515 mmol) of Phtu were suspended in 10 ml of diethilic ether and, at −70 °C, 0.32 ml (0.512 mmol) of a 1.6 M hexane solution of butyllithium were added. The clear and colourless solution was stirred and allowed to reach room temperature and 100 mg (0.514 mmol) of [{Rh(CO)$_2$Cl}$_2$] dissolved in 5 ml of Et_2O were then added. A red solution and a white precipitate (LiCl) formed. The IR spectrum of this solution showed four carbonyl bands at 2065m, 2024s, 1997m, 1970s cm^{-1}. To the solution was added 30 ml of THF, which was then refluxed and IR monitored until the disappearance of the two bands at 2065 and 1997 cm^{-1}. These two transient bands could be reasonably assigned to a thiolato-like bridged dinuclear complex, but it has been impossible to isolate this species even at low temperature. The solution was filtered on Celite and dried in vacuum to obtain an unstable dark red product. IR (KBr, cm^{-1}): 3358w br (νNH), 3058w 2958vw 2923vw (νCH), 2021vs 1966vs (νCO), 1590s 1551s (νNCN).

2.2.8. Preparation of $(EtO)_3Si(CH_2)_3NHC(S)NHPh$ (Siphtu)

In a 100 ml Schlenk flask 2 g (9.02 mmol) of $(EtO)_3Si(CH_2)_3NH_2$ and 1.22 g (9.02 mmol) of PhNCS were dissolved under nitrogen in 25 ml of dry ethanol. An exothermic reaction took place. The solution was then refluxed for 1 h and then the solvent completely evaporated under vacuum. The product is a pale yellow viscous liquid, giving satisfactory spectroscopic data [6].

2.2.9. Preparation of $(EtO)_3Si(CH_2)_3NCS$

The synthesis of this compound was performed following the published method with minor changes [7]. Hexane instead of diethyl ether was used to extract the liquid isothiocyanate that was subsequently obtained as a yellow oil, by filtering the suspension and evaporating the hexane under vacuum.

2.2.10. Preparation of p-$\{(EtO)_3Si(CH_2)_3NHC(S)NH\}_2(C_6H_4)$ (Siphenditu)

In a 100 ml Schlenk flask 1.5 g (13.87 mmol) of 1,4-phenylendiamine and 7.31 g (27.75 mmol) of $(EtO)_3Si(CH_2)_3NCS$ were refluxed in 50 ml of dry ethanol under nitrogen for 2 h. A white precipitate was formed. The solvent was then completely evaporated under vacuum and 30 ml of hexane were added. The suspension was filtered and washed again with hexane, to obtain a white solid. Yield 95%. Elemental analysis (calcd for $C_{26}H_{50}N_4O_6S_2Si_2$): C, 48.7 (49.2); H, 7.9 (7.9); N, 9.4 (8.8); S, 10.7 (10.0). ^{1}H NMR ($CDCl_3$, 300 MHz, δ/ppm): 7.9 (s, 2 H, C_6H_4NH); 7.29 (s, 4 H, C_6H_4); 6.38 (s, 2 H, CH_2NH); 3.79 (q, 12 H, CH_2O); 3.74 (m, 4 H, CH_2NH); 1.75 (m, 4 H, CH_2); 1.20 (t, 18 H, CH_3CH_2O); 0.82 (m, 6 H, CH_2Si). IR (KBr, cm^{-1}): 3250s sh 3190s br (νNH), 2975s, 2928m 2884m (νCH), 1552s 1538s 1522s (ν_{as}NCN, B band), 1103vs 1081vs br (νSiO), 643m (ν_sCS, G band).

2.2.11. Reaction of Siphenditu with $[\{Rh(cod)Cl\}_2]$, preparation of $[\{Rh(cod)Cl\}_2$(Siphenditu)] (5)

128.75 mg (0.2025 mmol) of Siphenditu were dissolved in 10 ml of CH_2Cl_2 under nitrogen and added to a solution of 100 mg (0.405 mmol) of $[\{Rh(cod)Cl\}_2]$ in 20 ml of dichloromethane. The solution was allowed to react for 1 h and then dried under vacuum. A yellow solid formed, which was washed with hexane and filtered. Yield 97%. Elemental analysis (calcd for $C_{42}H_{74}Cl_2N_4O_4Rh_2S_2Si_2$): C, 45.10 (44.72); H, 6.74 (6.61); N, 5.10 (4.97); S, 5.58 (5.68). ^{1}H NMR ($CDCl_3$, 100 MHz, δ/ppm): 11.3 (s, br, 2 H, C_6H_4NH); 7.2 (s, 4 H, C_6H_4); 6.1 (s, br, 2 H, CH_2NH); 4.2 (s, br, 8 H, CH=CH); 3.7 (q, 12 H, CH_2O); 3.5 (t, 4 H, CH_2NH); 2.44–2.39 (m, 8 H, CH_2, cod); 1.84, 1.76, 1.68, 1.62 (m, 8 H, CH_2, cod; CH_2CH_2Si); 1.14 (t, 18 H, CH_3); 0.55 (t, 4 H, CH_2Si). IR (KBr, cm^{-1}): 3274m, 3151m, (νNH), 2975m, 2928m, 2884m (νCH), 2832m (νCH, cod), 1558s 1521s (ν_{as}NCN, B band), 1101vs 1077vs (νSiO).

2.2.12. Preparation of $5SiO_2 \cdot SiO_{3/2}(CH_2)_3NHC(S)NHPh$ (XGphtu)

In a 100 ml beaker 3.22 g (9 mmol) of Siphtu and 9.4 g (45.1 mmol) of TEOS were dissolved in 25 ml of ethanol. 3 mg of NH_4F in 4 ml of water were added dropwise with stirring. Gelation occurred in less than 1 h. After 4–5 days the dried gel was crushed and washed with water, ethanol and ether, then dried under vacuum at 80 °C. Elemental analysis (calcd for $C_{10}H_{13}N_2O_{11.5}SSi_6$): C, 21.78 (22.00); H, 2.70 (2.40); N, 4.70 (5.13); S, 5.84 (5.87). IR (KBr, cm^{-1}): 3375br (νOH, νNH), 2937w (νCH), 1551m (ν_{as}NCN, B band), 1092vs br (νSiO). EDX atomic ratios: Si/S, 5.94. Surface area, BET: 91 m^2 g^{-1}.

2.2.13. Preparation $[SiO_{3/2}(CH_2)_3NHC(S)NHPh]_n$ (XGphtu)*

30 ml of ethanol, 2 g (18.15 mmol) of $[SiO_{3/2}(CH_2)_3NH_2]_n$, and 3 ml (20 mmol) of phenylisothiocyanate were introduced in a 100 ml Schlenk flask, and refluxed for 6 h. An ivory precipitate formed, and was filtered, washed with ethanol, ether and than dried in vacuum. Elemental analysis (calcd for $C_{10}H_{13}N_2O_{1.5}SSi$): C, 50.10 (48.95); H, 5.31 (5.34); N, 11.09 (11.41); S, 13.26 (13.06). IR (KBr, cm^{-1}): 3241s br (νNH), 3050m 2927m, 2873w (νCH), 1540s (ν_{as}NCN, B band), 1125vs 1025vs br (νSiO), 605m (νCS, G band). EDX atomic ratios: Si/S, 1.07. Surface area, BET: 0 m^2 g^{-1}.

2.2.14. Preparation of $\{p$-$[SiO_{3/2}(CH_2)_3NHC(S)NH]_2(C_6H_4)\}_n$ (XGphenditu)*

In a 100 ml flask, 573 mg (5.2 mmol) of $[SiO_{3/2}(CH_2)_3NH_2]_n$ were dissolved in 20 ml of 95% ethanol and a solution of 500 mg (2.6 mmol) of 1,4-phenylenediisothiocyanate in 20 ml of THF was added. The solution was allowed to reflux gently for 1 h. A white, powdery precipitate formed and was washed with ethanol, diethilic ether and then dried. Elemental analysis (calcd for $C_7H_{10}N_2O_{1.5}SSi$): C, 39.02 (40.75); H, 5.16 (4.88); N, 12.17 (13.58); S, 13.84 (15.54). IR (KBr, cm^{-1}): 3273m br (νNH), 2927m 2877m sh (νCH), 1545s br (ν_{as}NCN, B band), 1132vs 1037vs (νSiO). EDX atomic ratios: Si/S, 0.85. Surface area, BET: 0 m^2 g^{-1}.

2.2.15. Anchoring rhodium on functionalized xerogels and silsesquioxanes

In all cases rhodium complexes were anchored by stirring for some hours a suspension of thiourea-functionalized material (XGphtu, XGphtu* or XGphenditu*) with a solution in CH_2Cl_2 of an excess of $[\{Rh(cod)Cl\}_2]$ or $[\{Rh(CO)_2Cl\}_2]$. The solid was then filtered in the air and washed repeatedly with dichloromethane.

2.2.15.1. [{Rh(cod)Cl}$_2$] supported on XGphtu (Rh/XGphtu). IR (KBr, cm^{-1}): 3315s vbr (νNH, νOH), 3064w sh, 2937vw, 2883vw (νCH), 2832vw sh (νCH, cod), 1551s br (ν_{as}NCN, B band), 1129vs vbr (νSiO). EDX atomic ratios: Si/Rh 11, Rh/S 0.54, Rh/Cl 1.2. XPS atomic ratios: Si/Rh 12, Rh/S 1.2, Rh/Cl 0.9.

2.2.15.2. [{Rh(cod)Cl}$_2$] supported on XGphtu (Rh/XGphtu*).* IR (KBr, cm^{-1}): 3210m br (νNH), 3050w 2930w (νCH) 2999w sh 2829m (νCH, cod), 1550s br (ν_{as}NCN, B band), 1128vs 1020vs (νSiO). EDX atomic ratios: Si/Rh 2.15, Rh/S 0.5, Rh/Cl 1. XPS atomic ratios: Si/Rh 2, Rh/S 0.9, Rh/Cl 1.3.

2.2.15.3. [Rh(cod)Cl]$_2$ supported on XGphenditu (Rh/XGphenditu*).* IR (KBr, cm^{-1}): 3290m br (νNH), 2927w (νCH) 2995w sh 2830m (νCH, cod), 1546m 1511s (ν_{as}NCN, B band), 1130vs 1032vs (νSiO). EDX atomic ratios: Si/Rh 3.0, Rh/S 0.6, Rh/Cl 1.1.

2.2.15.4. [Rh(CO)$_2$Cl]$_2$ supported on XGphtu (RhCO/XGphtu). IR (KBr, cm^{-1}): 3400m vbr (νNH, νOH), 2937w (νCH), 2081s 2011s (νCO), 1552m br (ν_{as}NCN, B band), 1099vs vbr (νSiO).

2.2.15.5. [Rh(CO)$_2$Cl]$_2$ supported on XGphtu (RhCO/XGphtu*).* IR (KBr, cm^{-1}): 3241s br (νNH), 3050m 2927m, 2873w (νCH), 2074s 2000s (νCO), 1541s br (ν_{as}NCN, B band), 1125vs 1025vs br (νSiO).

2.2.15.6. [Rh(CO)$_2$Cl]$_2$ supported on XGphenditu (RhCO/XGphenditu*).* IR (KBr, cm^{-1}); 3291m br (νNH), 2927w (νCH) 2074s 2000s (νCO), 1545m 1511s (ν_{as}NCN, B band), 1129vs 1020vs (νSiO).

2.2.16. Hydroformylation reactions

In a typical run, distilled styrene (2 ml), toluene (3 ml) and the catalyst were introduced under nitrogen in the autoclave to achieve an approximate styrene/Rh ratio of 300, based on the EDX atomic Si/Rh ratio. After some pressurization and evacuation cycles at −20 °C, the autoclave was charged at room temperature with a 1/1 hydrogen/carbon monoxide mixture at 60 atm of pressure. The reaction mixture was stirred at 80 °C for 10–12 h, filtered in the air and analysed by GLC. The recovered catalyst was washed with dichloromethane to be re-used in a further run. For all the catalytic runs the styrene conversion was about 99% and the yield in the two isomeric *iso*- and *n*-aldehydes was about 98%. Trace amounts of ethylbenzene (< 1%) were sometimes detected. The same conditions were used for a homogeneous hydroformylation run using the model compound **1** as catalyst. Regioselectivity (*iso*/*n* aldehydes ratios) for each catalyst at the first run are: 2.2 (Rh/XGphtu), 0.9 (Rh/XGphtu*), 1.4 (Rh/XGphenditu*), 1.9 (compound **1**, homogeneous). Regioselectivity ratios after subsequent catalytic runs are reported in Fig. 8.

2.2.17. Reactions of Rh/XGphtu with N(C$_2$H$_5$)$_3$*

100 mg of Rh/XGphtu* were put in two autoclaves under the same conditions used for hydroformylation reactions (excluding styrene). The quantity of triethylamine was calculated on the formula $SiO_{3/2}(CH_2)_3NHC(S)NHPh \cdot \frac{1}{2}Rh(cod)Cl$, based on the EDX S/Rh ratio. In the first autoclave an excess (100 μl) of NEt_3 was added using a graduated micropipette; in the second autoclave 0.5 mol respect to rhodium (19 μl) was added. The autoclaves were heated to 80 °C for 10 h, the solids filtered in the air and washed with dichloromethane. IR spectra in the carbonyl region are reported in Fig. 7.

2.3. X-ray data collection, structure determination and refinement for [Rh(cod)(Phtu)Cl] · $\frac{1}{2}CH_2Cl_2$ (1 · $\frac{1}{2}CH_2Cl_2$) and Phenditu

Yellow crystals for X-ray analysis of **1** · $\frac{1}{2}CH_2Cl_2$ were obtained by precipitation with hexane from a dichloromethane solution of **1**. They were all of poor quality. Suitable colourless crystals of Phenditu were obtained by recrystallization from a methanol solution. The crystallographic data for both compounds are summarized in Table 1. Data were collected at room temperature (22 °C) on a Siemens AED diffractometer,

Table 1
Summary of crystallographic data for complex **1** · $\frac{1}{2}CH_2Cl_2$ and Phenditu

Formula	$C_{21}H_{24}ClN_2RhS \cdot \frac{1}{2}CH_2Cl_2$	$C_{14}H_{22}N_4S_2$
Mol. wt.	517.32	310.47
Crystal system	monoclinic	monoclinic
Space group	$P2_1/c$	$P2_1/a$
a (Å)	16.115(10)	9.294(3)
b (Å)	11.095(5)	7.963(3)
c (Å)	12.348(8)	11.004(5)
β (deg)	90.70(2)	91.94(2)
V (Å^3)	2208(2)	813.9(5)
Z	4	2
D_{calcd} (g cm^{-3})	1.556	1.267
$F(000)$	1052	332
μ(Cu K α) (cm^{-1})	94.30	29.25
θ range (deg)	3–70	3–70
Unique total data	4191	1630
Unique observed data [$I > 2\sigma(I)$]	2142	1239
GOF [a]	1.11	1.05
$R(F_o)$ [b]	0.0688	0.0757
$R(F_o)$ [c]	0.0861	0.0814

[a] $GOF = [\Sigma w(|F_o| - |F_c|)^2/(N_{observns} - N_{var})]^{1/2}$.
[b] $R = \Sigma||F_o| - |F_c||/\Sigma|F_o|$.
[c] $R_w = [\Sigma w(|F_o| - |F_c|)^2/\Sigma w(F_o)^2]^{1/2}$.

using the nickel-filtered Cu Kα radiation and the θ–2θ scan type. The reflections were collected with a variable scan speed of 4–12 deg min^{-1} and a scan width of $(1.20 + 0.142 \tan \theta)°$. One standard reflection was monitored every 100 measurements; no significant decay was noticed over the time of data collection. The individual profiles have been analysed following Lehmann and Larsen [8]. Intensities were corrected for Lorentz and polarization effects. A correction for absorption was applied; the maximum and minimum values for the transmission coefficient were 1.0000 and 0.6050 for **1** $\cdot \frac{1}{2}CH_2Cl_2$, 1.0000 and 0.6546 for Phenditu [9]. Only the observed reflections were used in the structure solution and refinement.

The structures were solved by direct and Fourier methods and refined by full-matrix least squares, first with isotropic thermal parameters and then with anisotropic thermal parameters for all non-hydrogen atoms (excepting for those of the dichloromethane molecule in **1** $\cdot \frac{1}{2}CH_2Cl_2$). All hydrogen atoms of **1** $\cdot \frac{1}{2}CH_2Cl_2$ (excepting those of the dichloromethane molecule) were placed at their geometrically calculated positions (C–H and N–H = 0.96 Å) and refined isotropically riding on the corresponding carbon or nitrogen atoms, whereas those of Phenditu were clearly localized in the final ΔF map and refined isotropically. In the final cycles of refinement a weighting scheme, $w = [\sigma^2(F_o) + gF_o^2]^{-1}$, was used; at convergence the g values were 0.0038 for **1** $\cdot \frac{1}{2}CH_2Cl_2$ and 0.0031 for Phenditu. The analytical scattering factors, corrected for the real and imaginary parts of anomalous dispersions, were taken from Ref. [10]. All calculations were carried out on the Gould Powernode 6040 and Encore 91 of the "Centro di Studio per la Strutturistica Diffrattometrica" del C.N.R., Parma, using the SHELX-76 and SHELXS-86 systems of crystallographic computer programs [11]. The final atomic coordinates for the non-hydrogen atoms are given in Tables 2 and 3. Additional data (atomic coordinates of the hydrogen atoms, thermal parameters) have been deposited or are available from the authors on request.

Table 2
Atomic coordinates ($\times 10^4$) and isotropic thermal parameters (Å$^2 \times 10^4$) for the non-hydrogen atoms of the complex **1** $\cdot \frac{1}{2}CH_2Cl_2$

Atom	x	y	z	U
Rh	1447.8(6)	2341.7(8)	4239.8(9)	426(3) [a]
Cl	2426(2)	3898(3)	4683(4)	678(14) [a]
S	2102(2)	666(3)	5129(3)	549(12) [a]
N(1)	2997(7)	107(9)	6895(10)	613(44) [a]
N(2)	3125(8)	2058(9)	6290(11)	639(47) [a]
C(1)	2798(8)	962(11)	6166(12)	527(48) [a]
C(2)	2753(8)	−1117(11)	6901(13)	558(51) [a]
C(3)	2443(9)	−1589(13)	7877(13)	613(57) [a]
C(4)	2262(10)	−2837(14)	7920(15)	716(63) [a]
C(5)	2390(10)	−3541(14)	7027(14)	683(65) [a]
C(6)	2687(10)	−3079(13)	6083(15)	642(61) [a]
C(7)	2875(9)	−1840(13)	5998(14)	627(58) [a]
C(8)	3695(7)	2433(12)	7089(13)	579(47) [a]
C(9)	3534(11)	3363(17)	7759(15)	798(73) [a]
C(10)	4099(13)	3778(20)	8520(16)	933(85) [a]
C(11)	4856(13)	3202(20)	8585(18)	1021(92) [a]
C(12)	5053(13)	2300(19)	7875(22)	1306(113) [a]
C(13)	4467(10)	1886(17)	7147(17)	888(78) [a]
C(14)	528(9)	3715(12)	3996(14)	590(57) [a]
C(15)	900(10)	3509(12)	3018(14)	585(56) [a]
C(16)	531(10)	2728(15)	2063(12)	852(67) [a]
C(17)	691(11)	1469(18)	2136(13)	830(73) [a]
C(18)	856(10)	994(13)	3306(13)	639(59) [a]
C(19)	363(8)	1218(11)	4174(12)	469(47) [a]
C(20)	−430(8)	1934(13)	4131(15)	668(61) [a]
C(21)	−302(11)	3288(14)	4323(13)	718(64) [a]
Cl(21)	5582(13)	481(18)	557(15)	1768(78)
Cl(22)	4425(9)	−806(13)	−837(12)	1073(43)
C(22)	4488(20)	348(31)	157(29)	1096(122)

[a] Equivalent isotropic U defined as one-third of the trace of the orthogonalized $\mathbf{U}_{ij}$ tensor.

Table 3
Atomic coordinates ($\times 10^4$) and equivalent isotropic thermal parameters (Å$^2 \times 10^4$) defined as one-third of the trace of the orthogonalized $\mathbf{U}_{ij}$ tensor, for the non-hydrogen atoms of Phenditu

Atom	x	y	z	U
S(1)	211(1)	521(2)	3061(1)	471(4)
N(1)	−2485(5)	1306(5)	2418(4)	476(13)
N(2)	−2111(4)	329(6)	4372(4)	478(13)
C(1)	−1571(5)	749(5)	3281(4)	376(12)
C(2)	−2055(6)	1765(9)	1198(5)	536(18)
C(3)	−3333(7)	1770(11)	318(5)	674(23)
C(4)	−2873(11)	1996(12)	−987(6)	826(31)
C(5)	−3581(5)	184(6)	4654(4)	393(13)
C(6)	−4058(6)	953(6)	5703(4)	458(14)
C(7)	−5463(6)	781(6)	6034(4)	480(15)

3. Results and discussion

3.1. Substituted thioureas and rhodium complexes

In order to have suitable molecular models to identify the tethered species, the 'model' thiourea ligands Phtu and Phenditu (Scheme 1) and their rhodium complexes were prepared. Phenditu is a new ligand and its solid state structure has been determined and is described below.

Phtu and Phenditu react with $[\{Rh(cod)Cl\}_2]$ and $[\{Rh(CO)_2Cl\}_2]$ giving the 1:1 rhodium/sulphur complexes [Rh(cod)Cl(Phtu)] (**1**), [$\{Rh(cod)Cl\}_2$(Phenditu)] (**2**), [Rh(CO)$_2$Cl(Phtu)] (**3**) [5] and [$\{Rh(CO)_2Cl\}_2$(Phenditu)] (**4**), characterized by IR, ^{1}H NMR and elemental analysis. The crystal structure of compound **1** was solved by an X ray structural analysis.

As regards the IR spectra, coordination through the sulphur atom normally causes the B band (ν_{as}NCN) [12]

of the thiourea group to undergo a slight shift to higher frequencies. More pronounced is the shift towards low frequencies of the G band (the band with the higher C=S stretching character). However, this band is difficult to detect unequivocally. In the ^{1}H NMR spectra the NH resonances move downfield by about 2 ppm, deshielding being probably due to coordination as well as to the formation of intramolecular hydrogen bonds with the chlorine atom (see the solid state structure of **1**, and those of related compounds in Refs. [1,5]). Compound **2** is insoluble in commonly available deuterated solvents, thereby preventing NMR characterization. The analogous compound **5**, with the thiourea ligand containing the $(EtO)_3Si$-group, is soluble in light alcohols and chlorinated solvents. The IR spectra of the complexes **3** and **4** show the two strong CO absorptions of the *gem*-$Rh(CO)_2$ fragment (**3**: 2070, 1998 cm^{-1}; **4**: 2072, 2000 cm^{-1}) shifted to lower frequencies compared to the starting dimer (2093, 2036 cm^{-1}) as expected [13].

By sol–gel processing the $(EtO)_3Si$-containing thiourea Siphtu and by reactions of $[SiO_{3/2}(CH_2)_3NH_2]_n$ oligomers with phenylisothiocyanate and 1,4-phenylenediisothiocyanate, three kinds of substance are produced. The first one (XGphtu) is a genuine xerogel obtained by co-processing Siphtu with TEOS (cross-linking agent). The second one (XGphtu*) should be regarded as a molecular substance, being a mixture of oligomeric species of formula $[SiO_{3/2}(CH_2)_3NHCSNHPh]_n$. The third one (XGphenditu*) is obtained, in a similar manner to XGphtu*, by reacting 1,4-phenylenediisothiocyanate with the $[SiO_{3/2}(CH_2)_3NH_2]_n$ oligomers, but this product should be again a polymeric material, reticulation being due to the thiourea linkages formed by the double isothiocyanate. In these substances the integrity of the thiourea functions is checked by comparing their IR spectra with those of the corresponding model compounds, in particular the B band. In the case of XGphtu* all the amino groups are probably converted to the thiourea function, as is suggested by the elemental analysis. In the case of XGphenditu* complete functionalization is probably not always achieved.

All the functionalized materials are able to bind the Rh(cod)Cl and $Rh(CO)_2Cl$ fragments, by suspending them in a CH_2Cl_2 solution of the respective rhodium precursors. The rhodium-containing solids Rh/XGphtu, Rh/XGphtu* and Rh/XGphenditu* are obtained from $[\{Rh(cod)Cl\}_2]$, RhCO/XGphtu, RhCO/XGphtu* and RhCO/XGphenditu* from $[\{Rh(CO)_2Cl\}_2]$. In no case was complete reaction between the thiourea functions and the rhodium moieties found, the EDX higher Rh/S ratio being about 0.5. The IR spectra do not show the presence of free thioureic functions, the B band being too large and the G band being too weak for detection. In the case of the rhodium-carbonyl species the two IR carbonyl bands (typical of the *gem*-$Rh(CO)_2$ fragment) found in the supported complexes are comparable to those of the model compounds. In the case of RhCO/XGphtu a shift of about 10 cm^{-1} towards higher frequencies is observed, compared to the oligomeric RhCO/XGphtu*. This could be due to the different polarity of the two supports, XGphtu being more polar than XGphtu* because of the presence of uncondensed Si–OH groups. The materials obtained from $[\{Rh(cod)Cl\}_2]$ were used as catalyst precursors, those obtained from $[\{Rh(CO)_2Cl\}_2]$ were used to compare their IR spectra with those of the species formed after the catalysis.

3.2. Description of the crystal structure of [Rh(cod)Cl(Phtu)] · ½CH_2Cl_2 (**1** · ½CH_2Cl_2)

In the crystals of **1** · ½CH_2Cl_2 complexes **1** and dichloromethane molecules of solvation are present. The structure of the complex **1** is shown in Fig. 1 together with the atomic labelling scheme. Selected bond distances and angles are listed in Table 4. The Rh atom is coordinated by a Cl atom, an S atom from the Phtu molecule and by the cod ligand, interacting through the two double bonds. If the midpoints of these double bonds, M(1) and M(2), are taken into account, the Rh atom displays a slightly distorted square planar coordination. The structure of **1** is strictly comparable with that of [Rh(cod)Cl(Hbztu)], in which the *N*-benzoyl-*N'*-propylthiourea (Hbztu) replaces the *N*,*N'*-diphenylthiourea [1]. The values of the Rh–S and Rh–Cl bonds in **1**, 2.397(4) Å and 2.397(4) Å respectively, are very close to those found in the Hbztu complex, 2.382(1) and 2.382(1) Å. In the thiourea moiety the value of C–S bond distance in **1**, 1.723(15) Å, is only slightly longer than in the Hbztu complex, 1.701(4) Å. The values of the C–N bond lengths are practically equal in **1**, 1.333(17) and 1.344(18) Å, as expected for symmetrical

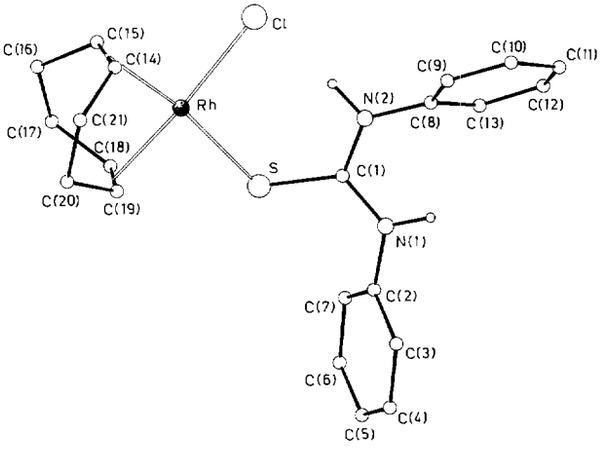

Fig. 1. View of the molecular structure of [Rh(cod)Cl(Phtu)] (**1**) together with the atomic numbering scheme.

Table 4
Selected bond distances (Å) and angles (deg) for complex $\mathbf{1} \cdot \frac{1}{2}CH_2Cl_2$

Rh–Cl	2.397(4)	C(14)–C(15)	1.37(2)
Rh–S	2.397(4)	C(18)–C(19)	1.36(2)
Rh–C(14)	2.144(14)	N(1)–C(1)	1.344(18)
Rh–C(15)	2.168(16)	N(2)–C(1)	1.333(17)
Rh–C(18)	2.110(15)	N(1)–C(2)	1.414(16)
Rh–C(19)	2.148(13)	N(2)–C(8)	1.403(19)
Rh–M(1)	2.044(15)	S–C(1)	1.723(15)
Rh–M(2)	2.017(14)		
M(1)–Rh–M(2)	87.2(6)	S–C(1)–N(1)	120.7(11)
S–Rh–M(1)	170.6(4)	S–C(1)–N(2)	120.8(10)
S–Rh–M(2)	84.4(4)	N(1)–C(2)–C(3)	117.5(12)
Cl–Rh–M(1)	88.8(4)	N(1)–C(2)–C(7)	120.6(12)
Cl–Rh–M(2)	174.9(4)	N(2)–C(8)–C(9)	121.9(14)
Cl–Rh–S	99.8(1)	N(2)–C(8)–C(13)	119.1(13)
Rh–S–C(1)	118.1(5)	N(1)–C(1)–N(2)	118.4(11)
C(1)–N(1)–C(2)	128.1(11)	C(1)–N(2)–C(8)	127.2(12)
C(3)–C(2)–C(7)	121.8(15)	C(9)–C(8)–C(13)	118.9(14)

M(1) and M(2) are the midpoints of the C(14)–C(15) and C(18)–C(19) double bonds respectively.

thioureas, whereas in the Hbztu complex they are different, 1.314(6) and 1.380(4) Å, because of the presence of a carbonyl group adjacent to one of the C–N double bonds. Also, in complex **1** an intramolecular hydrogen bond is formed by the thioureic N(2) atom with the coordinated Cl atom (N(2)...Cl = 3.052(12) Å, N(2)–H–Cl = 173°).

3.3. Description of the crystal structure of Phenditu

The molecular structure of 1,4-bis(propylthiourea)benzene (Phenditu) is shown in Fig. 2 together with the atomic labelling scheme. Selected bond distances and angles are listed in Table 5. The molecule has an imposed crystallographic C_i symmetry, with the benzene ring lying-on the centre of symmetry.

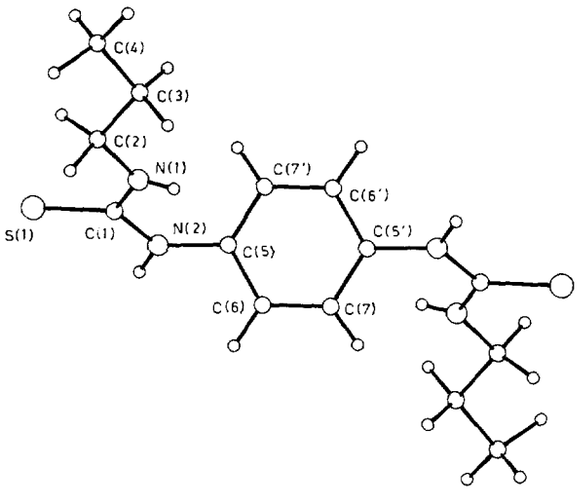

Fig. 2. View of the molecular structure of Phenditu together with the atomic numbering scheme.

Table 5
Selected bond distances (Å) and angles (deg) for Phenditu

N(1)–C(1)	1.330(6)	C(2)–C(3)	1.507(8)
N(1)–C(2)	1.460(7)	C(3)–C(4)	1.523(10)
N(2)–C(5)	1.416(6)	C(5)–C(6)	1.392(7)
N(2)–C(1)	1.358(6)	C(6)–C(7)	1.375(7)
S(1)–C(1)	1.691(5)	C(5)–C(7')	1.381(7)
C(2)–N(1)–H(1)	121(4)	C(1)–N(1)–H(1)	114(4)
C(1)–N(1)–C(2)	123.5(4)	C(1)–N(2)–C(5)	127.0(4)
C(5)–N(2)–H(2)	118(4)	C(1)–N(2)–H(2)	115(4)
S(1)–C(1)–N(2)	119.6(3)	S(1)–C(1)–N(1)	122.6(4)
N(1)–C(1)–N(2)	117.8(4)		

In the thioureic group, the C–S (1.691(5) Å) and C–N (1.330(6) and 1.358(6) Å) bond lengths are in agreement with those found in other substituted thioureas (average values 1.681(20) Å and 1.346(23) Å respectively, from Cambridge Crystallographic Data Centre). The thioureic groups are tilted with respect to the benzene ring by 56.6(2)°. An intermolecular hydrogen bond joins the molecules in chains (N(2)–H(2)...S(1)($-x, -y, -z+1$) = 3.349(4) Å, H(2)–S(1)($-x, -y, -z+1$) = 2.47(6) Å; N(2)–H(2)–S(1) = 164(5)°).

3.4. Hydroformylation reactions

All the rhodium-containing hybrid materials showed a high activity in the hydroformylation of styrene, at 80 °C and 60 atm of a 1/1 mixture of CO/H_2. The Rh(cod)Cl-containing solids were preferred as catalyst precursors because of the higher stability of this rhodium moiety, with respect to the analogue dicarbonyl fragment, allowing their storage in the air at room temperature. Styrene was completely converted in the branched (*iso*-) and linear (*n*-) aldehydes. No hydrogenation reactions took place, only traces of ethylbenzene having been detected and no alcohols were formed. The catalysts can be easily recovered by filtration in the air, and re-used in another catalytic run without loss of activity. The selectivity ratio (*iso*/*n*) at the first catalytic run for each catalyst is in the range 0.5–2.5, comparable with the value found using compound **1** as homogeneous catalyst (1.9).

During the catalytic reactions the starting cod-complex is converted into at least two carbonyl species present in each of the three catalysts after the catalytic runs, similar to the previously reported Rh/XGbztu and Rh/XGbztu* systems [1]. In the case of XGphtu*, the IR spectrum after the first catalytic run (Fig. 3(b)) shows the two bands of the supported $Rh(CO)_2Cl$(thiourea) *cis*-dicarbonyl complex found in RhCO/XGphtu* (Fig. 3(a)) together with other two bands shifted to lower frequencies. After three catalytic runs (Fig. 3(d)) the latter appear stronger whereas the

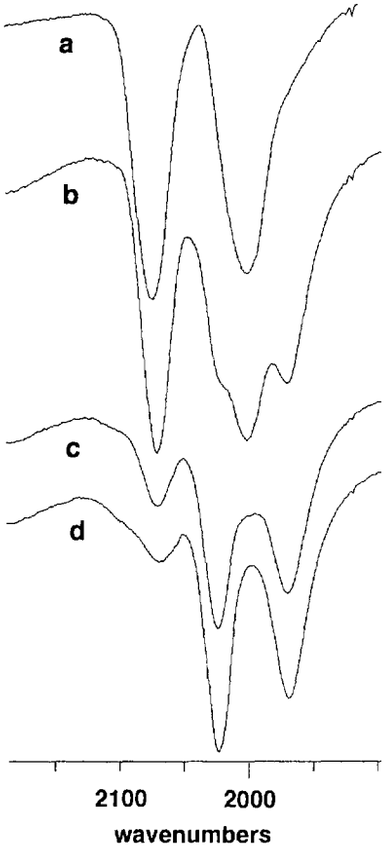

Fig. 3. IR spectra (KBr pellets) of: (a) RhCO/XGphtu*; (b) Rh/XGphtu* after the first catalytic run; (c) after two catalytic runs; (d) after three catalytic runs.

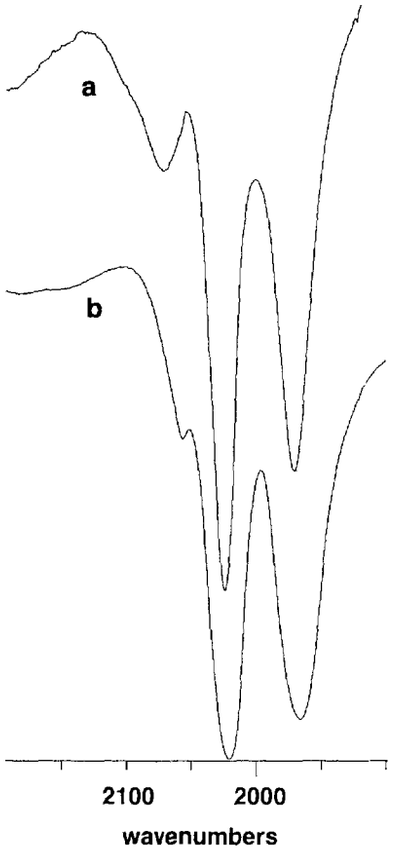

Fig. 4. (a) IR spectra (KBr pellets) of Rh/XGphtu* after three catalytic runs; (b) IR spectra (THF solution) of the thioureato complex [Rh(CO)$_2${PhNC(S)NHPh}].

former are reduced. As in the case of Rh/XGbztu and Rh/XGbztu* [1] the lower-frequency bands are attributable to a thioureato complex (Scheme 2(b)) which could derive from the complex HRh(CO)$_2$(thiourea) (Scheme 2(c)) by elimination of hydrogen. This hydrido complex, probably formed by oxidative addition of H_2 to the carbonyl-chloride complex (obtained by substitution of cod with CO; Scheme 2(a)) followed by reductive elimination of HCl, should be regarded as the active catalytic species. At the end of the reaction, the hydrido ligand can react with the acidic hydrogen of the –NHPh group, giving the thioureato species. Another possibility for the thioureato formation is the direct elimination of HCl (Scheme 2).

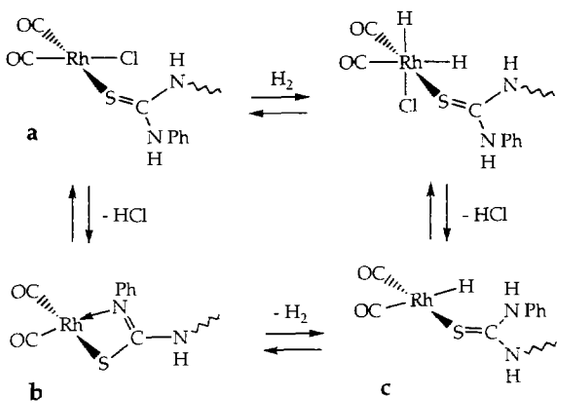

Scheme 2.

A model thioureato complex was prepared in solution reacting [(Rh(CO)$_2$Cl)$_2$] with Li[PhNC(S)NHPh]. Its CO stretching bands (Fig. 4(b)) match well those found in Rh/XGphtu* after the third catalytic run (Fig. 4(a)).

Other indirect evidence for the formation of a thioureato species was obtained by reacting Rh/XGphtu* with triethylamine under the hydroformylation conditions (80 °C, 60 atm of 1/1 H_2/CO, toluene) but without styrene. The IR spectra of the carbonyl species formed after this treatment are reported in Fig. 5. Using a lack of triethylamine (NEt_3/Rh = 0.5) results in the formation of four carbonyl bands (Fig. 5(b)) corresponding to those found in Rh/XGphtu* after the first catalytic run (Fig. 5(a)). On the other hand, the use of an excess of triethylamine gives rise to only one carbonyl species whose bands (Fig. 5(c)) correspond exactly to those of Rh/XGphtu* after three catalytic

runs (Fig. 5(d)). The same treatment in the absence of triethylamine gave only substitution of cod by two CO ligands.

For Rh/XGphenditu* and Rh/XGphtu a similar IR behaviour is observed (Figs. 6 and 7), but both rhodium species (chloride and thioureato) are present, even after three (Fig. 6(c)) and ten runs (Fig. 7(e)) respectively. Moreover, in the case of Rh/XGphenditu* the thioureato bands are prevalent after the first catalytic run whereas the chloride bands are stronger after the second run, suggesting an equilibrium between the two species.

For Rh/XGphtu and Rh/XGphenditu* a change in regioselectivity was observed when the catalysts were re-used (as it was for Rh/XGbztu [1]). The selectivity variation is depicted in Fig. 8. The collected data suggest that the selectivity change could be due to the fact that the amount of rhodium is lowered drastically on the surface, in such a way that the hydroformylation reaction 'moves' to the inside of the material, experiencing a different matrix environment. This hypothesis is based on the comparison between XPS and EDX analytical data, considering also the morphology of the surface and the IR data.

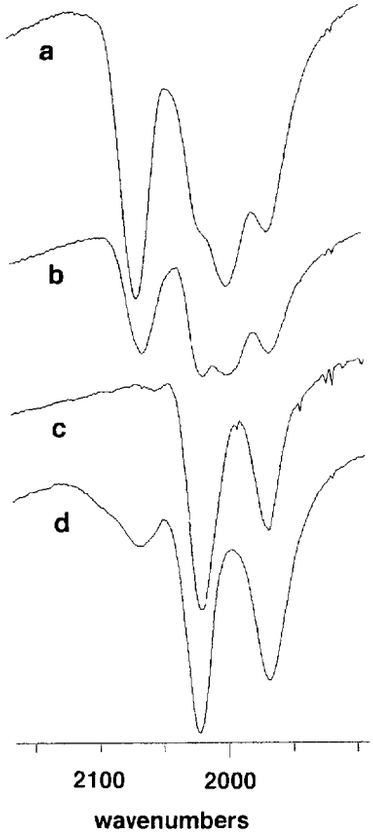

Fig. 5. IR spectra (KBr pellets) of: (a) Rh/XGphtu* after one catalytic run; (b) Rh/XGphtu* treated with 0.5 mole NEt_3; (c) Rh/XGphtu* treated with an excess of NEt_3; (d) Rh/XGphtu* after three catalytic runs.

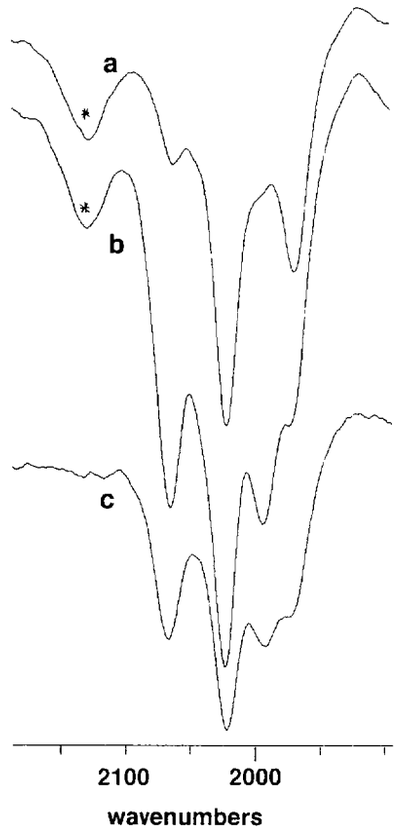

Fig. 6. IR spectra (KBr pellets) of Rh/XGPhenditu*; (a) after one catalytic run; (b) after two catalytic runs; (c) after three catalytic runs. (In the figure * denotes an isothiocyanate impurity.)

We investigated fully the case of the Rh/XGphtu and Rh/XGphtu* catalysts. The surface of the XGphtu support appears to be constituted of spheroidal aggregates of average diameter of 150 nm, as shown in the AFM image of Fig. 9 obtained for a small glassy monolith, and as previously found for other silica hybrid xerogels [14]. Consequently, XPS should probe the surface of these spheres (photoelectrons coming from an average depth of 5 nm), whilst EDX (with photons coming from an average depth of 1000 nm) gives a bulk analysis of the material.

XPS BE values are reported in Table 6, while XPS and EDX atomic ratios are reported in Table 7. From a comparison of the Rh3d BEs of the catalyst precursor Rh/XGphtu, the catalyst after five runs and after ten runs, we can exclude a strong electronic state modification on the surface Rh atoms notwithstanding the thiourea–thioureato transformation (Fig. 10). We can assign to Rh a +1 oxidation state, on the basis of the literature reports [15], while Cl2p BEs are compatible with Rh–Cl complex species. It is interesting to note that the Rh/Cl surface (XPS) and bulk (EDX) ratios remain closely comparable along the catalytic runs.

The S2p BEs (163 eV) clearly show the formation of

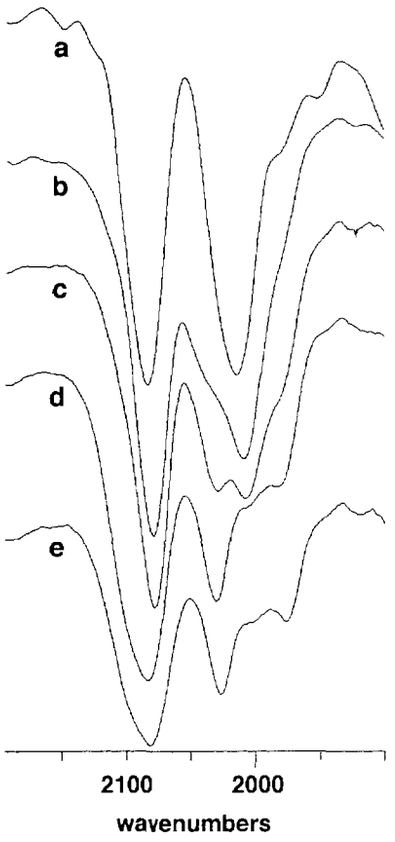

Fig. 7. IR spectra (KBr pellets) of: (a) RhCO/XGphtu; (b) Rh/XGphtu after the first catalytic run; (c) after the second run; (d) after the fifth run; (e) after the tenth run.

the Rh–S bond. Strongly oxidized S species (169 eV), as a sulphate, are present in a limited amount after the fifth run and clearly seen after the tenth. In the precursor, the Rh/S surface ratio is 1.2 and the bulk Rh/S ratio is 0.5. It appears that all the surface thioureic

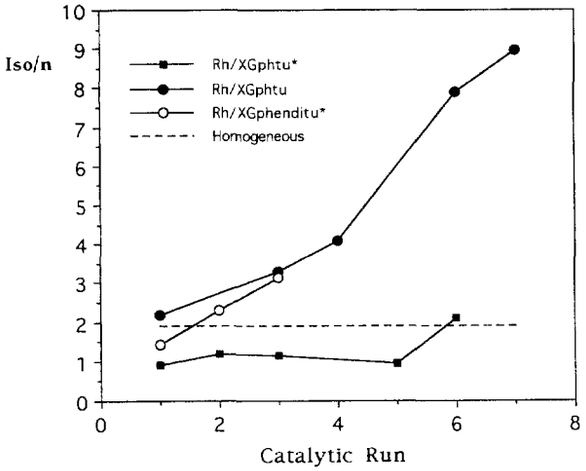

Fig. 8. *Iso/n* regioselectivity ratio vs. catalytic run number in the hydroformylation of styrene catalysed by Rh/XGphtu*, Rh/XGphtu, Rh/XGphenditu* and complex **1**.

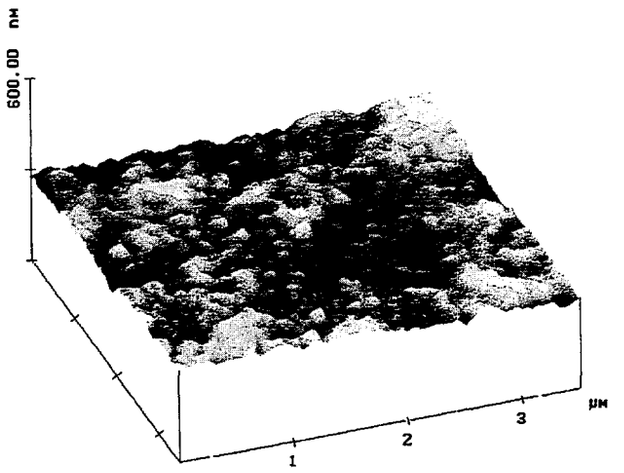

Fig. 9. AFM image of the surface of a monolith of XGphtu.

groups are coordinated by the metal but that internal groups are not all reachable by diffusion inside the xerogel. It must be noticed that the XPS Rh/S > 1 could be due to experimental error as well as to the formation of binuclear sulphur-bridged complexes [5]. The bulk experimental Si/S ratio (5.9) is in agreement with the nominal ratio (6) but the surface ratio is much higher (14.4). A sure explanation is not possible without further investigation on the sol–gel formation of XGphtu but, probably, the external part of the spheres contains preferentially Q silica atoms (Si atoms bound to four oxygen atoms, derived from TEOS condensation) respect to T silica atoms (bound to three oxygen atoms and the thiourea fragment). It has been reported that T species hydrolyse faster than Q species [16], consequently the internal part of the spheres, formed earlier during the sol–gel process, is probably richer in T silicon atoms than the external. We can imagine that the catalyst precursor is formed by spheroidal aggregates, poorer in sulphur on the surface than inside, with

Table 6
XPS BE (±0.2 eV) for Rh/XGphtu and Rh/XGphtu* before the catalysis and after different catalytic runs

Material	Cat. run	Rh(3d5/2)	S(2p) [a]	Cl(2p)
XGphtu	—	—	162.4	—
Rh/xGphtu	—	309.2	163.5	199.0
	5	309.25	163.45	199.3
			169.3 (traces)	
	10	309.2	163.5	199.1
			169.3	
XGhtu*	—	—	162.5	—
Rh/XGphtu*	—	309.0	163.1	198.9
	1	309.1	163.0	198.6
	6	309.0	162.5	198.5

[a] S(2p) BE for *N*-phenyl-*N'*-propylthiourea: 162.3 eV.

Table 7
EDX and XPS atomic ratios for Rh/XGphtu and Rh/XGphtu* before the catalysis and after different catalytic runs

Material	Cat. run	Si/Rh		Rh/S			Rh/Cl	
		EDX	XPS	EDX	XPS		EDX	XPS
					(S_{163})	(S_{tot})		
Rh/XGphtu	—	11.0	12.0	0.54		1.2	1.2	0.9
	1	12.5	n.a.	0.38		n.a.	0.8	n.a.
	5	13.0	33.0	0.40	1.35	1.15	0.9	0.8
	10	21.0	53.0	0.27	0.95	0.6	0.65	0.7
Rh/XGphtu*	—	2.15	2.0	0.50	0.9		1.0	1.3
	1	3.9	1.65	0.42	1.4		0.7	1.3
	6	3.3	10.0	0.60	1.1		1.1	0.95

n.a. = not available.

all the surface thiourea coordinated to the metal, and with a low inner concentration of rhodium.

After five catalytic runs the surface Si/Rh ratio rises to 33, owing to some surface Rh leaching, while the bulk ratio is practically unchanged (13). Correspondingly, the new sulphate species begins to appear in the XPS spectra at 169.3 eV (similar to the case of XGbztu [1]). It appears clearly that decomposition of the complex has occurred to a certain extent, but the $Rh/S_{163.5}$ ratio (1.35) suggests that all the thioureic sulphur remains bonded to rhodium. The sulphate is probably formed during the exposure to the air after the catalysis, by oxidation of finely dispersed elemental sulphur, coming from thiourea decomposition.

After ten catalytic runs the surface Si/Rh ratio rises to 53 but the catalyst is still active, even if also the bulk rhodium content is decreased (Si/Rh = 21). The $Rh/S_{163.5}$ ratio is still 0.95, indicating that metal leaching is probably due to the decomposition of the thiourea function, not simply to the breaking of the coordinative Rh–S bond. The Rh/S total ratio is 0.59, suggesting that rhodium is lost in the reaction medium.

In the case of Rh/XGphtu* the XPS BEs are similar to Rh/XGphtu, confirming an analogous coordinative situation. Also in this case, there is not a strong electronic state modification on the Rh atoms, as the Rh3d bands are well comparable before and after the catalytic runs. Regarding the catalytic behaviour, there is no regioselectivity variation in the first catalytic runs (Fig. 8), but a strong bulk rhodium leaching is observed (Si/Rh, 2.15 in the starting material, 3.9 after the first run), contrary to that found for the diluted system. This situation suggests that in Rh/XGphtu* rhodium thiourea complexes are not 'protected' by a polymeric network, and that there is not a well-defined 'surface'. In fact the XPS atomic ratios do not show any trend. Actually, in the formation of XGphtu glassy monoliths are obtained, whereas XGphtu* is constituted by a fine powdery precipitate and should be regarded as a molecular solid. Moreover, no formation of oxidized sulphur species was observed, probably because the decomposed thiourea fragments were lost in the reaction medium, and were not trapped in the matrix as observed for Rh/XGphtu.

The Rh/XGphenditu* material was not analysed by EDX or XPS after the catalysis, but its catalytic behaviour is similar to that of Rh/XGphtu, suggesting that also in this case the polymeric nature is probably responsible for the regioselectivity change.

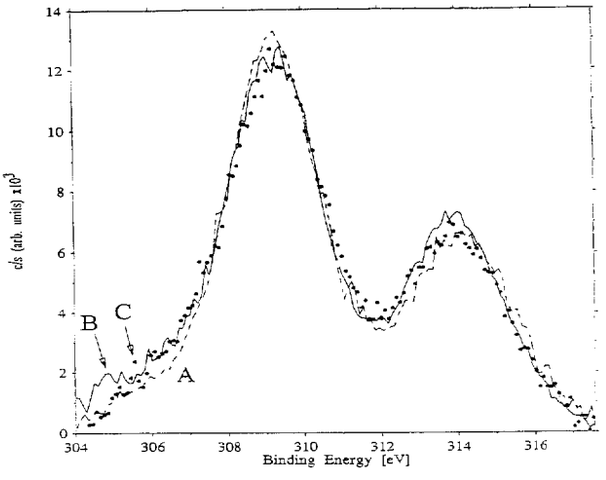

Fig. 10. X-ray photoelectron spectra in the Rh3d region for: (A) Rh/XGphtu; (B) sample A after five catalytic runs; (C) sample A after ten catalytic runs.

4. Conclusions

The comparison between EDX and XPS data suggests that for Rh/XGphtu the active complex is depleted from the surface of the spheroidal aggregates, while it is much more protected inside the particles. The change in selectivity can be ascribed to the disappearance of the catalytic centres from the surface, where they show a regioselectivity similar to the homogeneous catalyst, in such a way that the predominant active species become the inner complexes which experience different environments, being immersed in solid–liquid interphases. A similar improvement in regioselectivity was recently found in the 1-hexene hydroformylation catalysed by zeolite-encapsulated Rh(I) species [17].

We can reasonably exclude that the thioureato species is responsible for this selectivity change for the following reason: for Rh/XGbztu the formation of the thioureato complex was complete after the first run and the selectivity changed also from the fourth to the fifth

cycles [1]. The thioureato is formed also in Rh/XGbztu* [1] and in Rh/XGphtu*, but the selectivity remains almost constant. These two catalysts are molecular materials, without an extended polymeric tridimensional framework.

The change in selectivity was also observed, even if not to the same extent, for Rh/XGphenditu*. This catalyst should behave similarly to Rh/XGphtu* and Rh/XGbztu* (it has been obtained in the same way) but in fact behaves like a polymeric matrix, as in this case the double isothiocyanate used to prepare XGphenditu* allows the formation of a cross-linked polymer.

In order to gain an insight into the textural features of these xerogels and consequently to better understand their matrix effects on the selectivity of this reaction, small angle neutron scattering measurements are being performed.

Acknowledgements

Financial support from CNR (Rome), Progetto Finalizzato Chimica Fine II and from MURST (Rome) is gratefully acknowledged. The facilities of Centro Interdipartimentale Misure (University of Parma) were used for recording NMR spectra and AFM images. The SEM at the Institutes of Petrology, Mineralogy and Geology, University of Parma, was used for EDX analysis. We gratefully thank the "Servizio ESCA" of the CNR in Montelibretti (Rome) for use of the XPS machine. The invaluable assistance of Dr. G. Righini in obtaining the XPS spectra is also acknowledged.

References

[1] D. Cauzzi, M. Lanfranchi, G. Marzolini, G. Predieri, A. Tiripicchio, M. Costa, R. Zanoni, J. Organomet. Chem. 488 (1995) 115.
[2] C. Sanchez, F. Ribot, New. J. Chem. 18 (1994) 1007.
[3] L.L. Hench, J.K. West, Chem. Rev. 90 (1990) 33. C.J. Brinker, G.W. Scherer, Sol–Gel Science, Academic Press, 1990.
[4] R.H. Grubbs, Chemtech (1977) 513. U. Schubert, New J. Chem. 18 (1994) 1049.
[5] D. Cauzzi, M.A. Pellinghelli, G. Predieri, A. Tiripicchio, Gazz. Chim. Ital. 123 (1993) 713.
[6] C. Ferrari, G. Predieri, A. Tiripicchio, M. Costa, Chem. Mater. 4 (1992) 243.
[7] T. Yamamoto, S. Sugiyama, K. Akimoto, K. Hayashi, Org. Prep. Proced. Int. 24 (1992) 346.
[8] M.S. Lehmann, F.K. Larsen, Acta Crystallogr. Sect. A: 30 (1974) 580.
[9] N. Walker, D. Stuart, Acta Crystallogr. Sect. A: 39 (1983) 158. F. Ugozzoli, Comput. Chem. 11 (1987) 109.
[10] International Tables for X-Ray Crystallography, vol. IV, Kynoch Press, Birmingham, UK, 1974.
[11] G.M. Sheldrick, SHELX-76 Program for Crystal Structure Determination, University of Cambridge, UK, 1976; SHELXS-86 Program for the Solution of Crystal Structures, University of Göttingen, 1986.
[12] K.A. Jensen, P.H. Nielsen, Acta. Chem. Scand. 20 (1966) 597.
[13] R.P. Hughes, in: G. Wilkinson, F.G.A. Stone, E.W. Abel (Eds.), Comprehensive Organometallic Chemistry, vol. 5, Pergamon, Oxford, 1983, pp. 285, 290.
[14] K.J. Shea, D.A. Loy, O. Webster, J. Am. Chem. Soc. 114 (1992) 6700.
[15] D. Briggs, M.P. Seah, Practical Surface Analysis by Auger and X-ray Photoelectron Spectroscopy, vol. 1, Wiley, London, 2nd edition, 1990.
[16] F. Babonneau, J. Maquet, J. Livage, Chem. Mater. 7 (1995) 1050.
[17] J.M. Andersen, A.W.S. Currie, J. Chem. Soc. Chem. Commun. (1996) 1543.